

# Experimental Study of Metal Bipolar Plate Microchannels Fabrication Using the Through Mask Electrochemical Machining

Shuangqing Qian\*, Yuanyuan Wu, Kai Bao, Yidan Zhou, Hongbei Cao, Hua Zhang

School of Mechanical Engineering, Nantong University, Nantong 226019, P. R. China

\*E-mail: [sqqian@ntu.edu.cn](mailto:sqqian@ntu.edu.cn)

Received: 19 April 2019 / Accepted: 11 June 2019 / Published: 5 August 2019

---

In this investigation, the through mask electrochemical machining (TMEMM) is used to generate micro-channel structures on metal bipolar plates. By taking serpentine flow channels fabrication as an example, the experiment system of the electrochemical machining is designed and built to evaluate the effect of machining parameters such as machining time and current density on the morphology of the flow channel. The experimental results show that the TMEMM can be utilized to process micro-channels on metal surfaces effectively and the island morphologies inside of the flow channels can be removed with increased machining time. Moreover, the machining efficiency and localization can be further improved by selecting a pulse voltage between 20V and 30V.

---

**Keywords:** through mask electrochemical machining; current density ; micro-channel; metal bipolar plate

## 1. INTRODUCTION

The bipolar plate is one of the key components in the proton exchange membrane fuel cells (PEMFC). In comparison with the graphite and some composite materials, metal materials have many advantages in their inherent properties such as good thermal and electrical conductivity and high density, and can be processed into very thin PEMFC bipolar plates (thickness < 150 μm) [1-3]. Moreover, metal bipolar plates can be easily machined in mass production and thus metal materials are very promising materials for bipolar plates [4, 5]. Because of the good mechanical properties of the metal material and their capabilities to be machined into very thin bipolar plates with miniature flow channels, the metal material has become one of the primary focus materials for bipolar plates in the future, which has attracted a lot of attentions from domestic and international researchers [6].

Currently, the primary forming processes for flow channels in metal bipolar plates include

molding, stamping and laser forming methods. With the miniaturization of fuel cells, those traditional machining methods become more and more difficult to produce satisfactory thin metal bipolar plates with micro channels in micro fuel cells. The Fuel Cell Center at Yuan Ze University[7,8] used both the electrochemical machining (ECM) and the electro discharge machining (EDM) on stainless steel (SS304) sheets, and successfully processed serpentine multi-flow channels with a width at 500 $\mu\text{m}$ , a depth at 200 $\mu\text{m}$  and 600 $\mu\text{m}$ , respectively. The electrochemical micro-machining (EMM) process is a non-contact process, involving no cutting force or flanging and therefore it is irrelevant to the material hardness and strength, which results in no material properties change after processing [9-11]. Liu[12] got micro holes and channels by electrochemical milling with micro spherical electrode. In order to improve the EMM process efficiency, Madore[13] proposed the through mask electrochemical machining (TMEMM) method to process thousands of micro pits simultaneously with diameters at tens to hundreds micrometers and depths at a few micrometers to dozens of micrometers on the surface of the metal within several seconds to a few minutes. Chen[14] used a polydimethylsiloxane (PDMS) mask during TMEMM for generating high-quality micro-dimple arrays. Qu[15, 16] also used this method to process array micro pits on the cylindrical surfaces and reduced the interelectrode gap to zero to get higher depth- width ratio. Instead of using the photoetching process, some researchers also used mobile mask in the electrochemical machining method to generate micro pits or holes [17, 18]. The modified TMEMM technology, in which the mask can be moved and reused, is based on the photoetching method, which can be used to process any conductive metal material with no restrictions on its stiffness, strength and toughness. However, when this method is used to process the micro channels, the mask is prone to displacement.

In this study, considering the facts of no tool wear or heat affected layers in work pieces, the TMEMM is used to machine serpentine flow channels in metal bipolar plates. The experimental study on the serpentine flow channels (multichannels) machining was carried out to study the influence of various machining parameters on the flow channel forming. The developed technology is able not only to solve the difficult issues of forming small size flow channels but also to greatly improve the machining efficiency by forming multiple flow channels simultaneously. Thus, the TMEMM shall have a very broad application prospect for machining metal double-surfaced flow channels.

## **2. EXPERIMENTAL SYSTEM AND ANODE SAMPLE PREPARATION**

### *2.1 Experimental system for electrochemical machining*

The TMEMM in bipolar plates is a special electrochemical machining method based on photolithography and its entire machining process can be illustrated by the schematic diagram shown in Figure 1. The surface of metal plates is coated with a photoresist layer with hollowed flow channel patterns after photolithography. After TMEMM is carried out, photoresist is then removed and metal bipolar plates with microchannels are finally made.

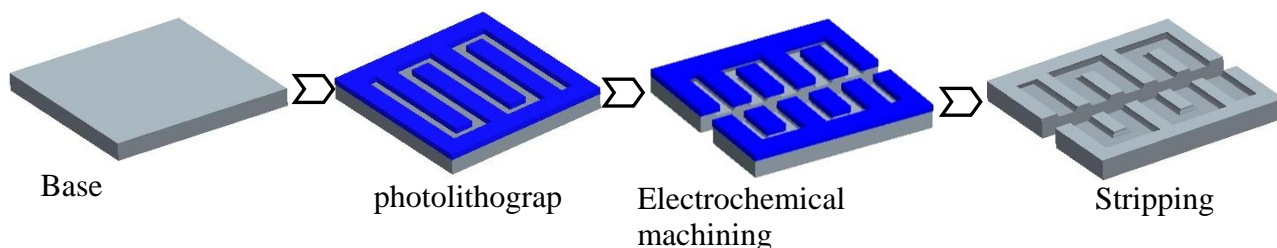
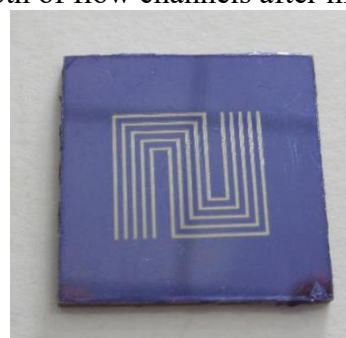
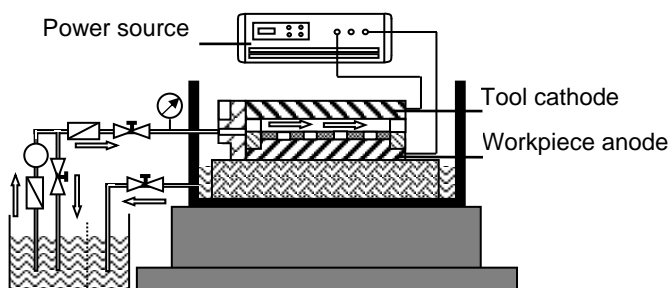


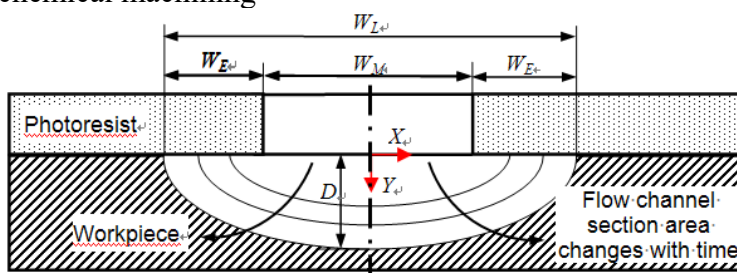
**Figure 1.** Flow Chart of machining metal microchannels using the TMEMM

The TMEMM experimental system for microchannels machining consists primarily of an electrolytic bath, an electrolyte circulation system, experimental clamping fixtures and a power supply system, as shown in the schematic diagram in Figure 2(a). The clamping fixtures material in the enclosed cathode and anode machining region requires strong etching resistance property and thus polymethyl methacrylate (PMMA) is selected in this experiment study. Inside the clamping fixtures, the electrolyte flow pattern is a lateral flow pattern. RSNP-4050 is used in the test as the single pulse power source with a maximum voltage output at 40V, and a maximum current output at 50A. During the pulse test, the duty ratio of the pulse voltage is kept at 50% and the frequency at 2 kHz. The electrolyte used in the test is neutral electrolyte  $\text{NaNO}_3$  solution with 10% density, and the reaction temperature is controlled at about  $30^\circ\text{C}$  during the electrochemical machining process. The electron scanning microscope (SEM, Hitachi S-3400N) and the 3D topography instrument (DVM500, Germany) are used to obtain the cross-section morphology of flow channels and to measure the width and depth of flow channels after machining.



(a) Schematic diagram of the experimental system for the electrochemical machining

(b) Anode sample after photoetching



(c) Schematic of the cross-section of the flow channels

**Figure 2.** Experimental system

## 2.2 Anode sample preparation

In this experimental system, the anode is made of a stainless steel (SUS304) and the sample dimension is 20mm×20mm×1mm (L×W×H). After ultraviolet photoetching, the thickness of the insulation layer of the workpiece anode is 50µm and the width of the hollowed flow channels on the insulation layer is 200µm. The overall morphology of the anode after photoetching is shown in Figure 2(b).

## 2.3 Evaluation criterion of the experimental results

During the initial stage of the flow channels machining using the TMEMM, the anode material dissolving occurred only in the vertical direction since those regions were not protected by the insulation layer, as illustrated in Figure 2(c). The electrolyte was filling in the entire machining gap between the electrodes and some of the anode material was dissolved in the horizontal direction with progressing which resulted in the actual width ( $W_L$ ) of the flow channel greater than the width ( $W_M$ ) in the insulation layer. It is called lateral corrosion, which will reduce the dimensional accuracy in TMEMM. In general, in order to improve the machining localization and the dimensional accuracy during the electrochemical machining, the side etching rate in the horizontal direction should be minimized while the etching rate in the depth direction should be maximized.

The etching factor ( $EF$ ) was used in this study as an index for evaluating the localization of the microchannels machining using the TMEMM, which is defined by:

$$EF = D / W_E = 2D / (W_L - W_M) \quad (1)$$

Where  $D$  is the depth of the flow channel;  $W_E$  is the side etching width;  $W_L$  is the width of the cross-section of the machined flow channel and  $W_M$  is the flow channel width in the insulation layer.

As shown in the above equation, the larger the calculated etching factor is after flow channel machining in the anode, the better the locality is.

## 3. RESULTS AND DISCUSSION

### 3.1 Influence of machining time on the Flow channel morphology

The machining time is an important machining parameter in controlling the depth and width of the flow channels in the anode during the electrochemical machining process. The effect of the machining time on the cross-section morphology of the flow channel is analyzed both by the simulation and the experiment.

By analyzing the changing trend of the current density distribution with the time on the flow channel surfaces, as shown in Figure 3(a), it is observed that the current density is lower in the central region and higher near both ends of flow channels at 10s and after that, the current density is gradually increasing in the central region and is gradually decreasing near the ends. The cross-section morphologies of the flow channel from the simulation at 10s and 40s are shown in Figure 3(b). It is seen from Figure 3(b) that the convex shapes appear in the cross-section of the central enclosed region at 10s; and the convex shapes disappear while the required grooved cross-section shapes appear at 40s.

According to the electrochemical machining theory, the material dissolving rate is proportional to the current density. At 10s, since the current density at the edges of both sides of the groove is higher than that in the central enclosed region, the dissolving rate at the edges of the groove is much higher than that in the central region, which results in the isolated island phenomena. After 20s, however, as the current density is gradually decreasing at both ends and is gradually increasing in the central region, the dissolving rate is also increasing and the isolated island phenomena is gradually disappearing, which leads to a stable machining stage.

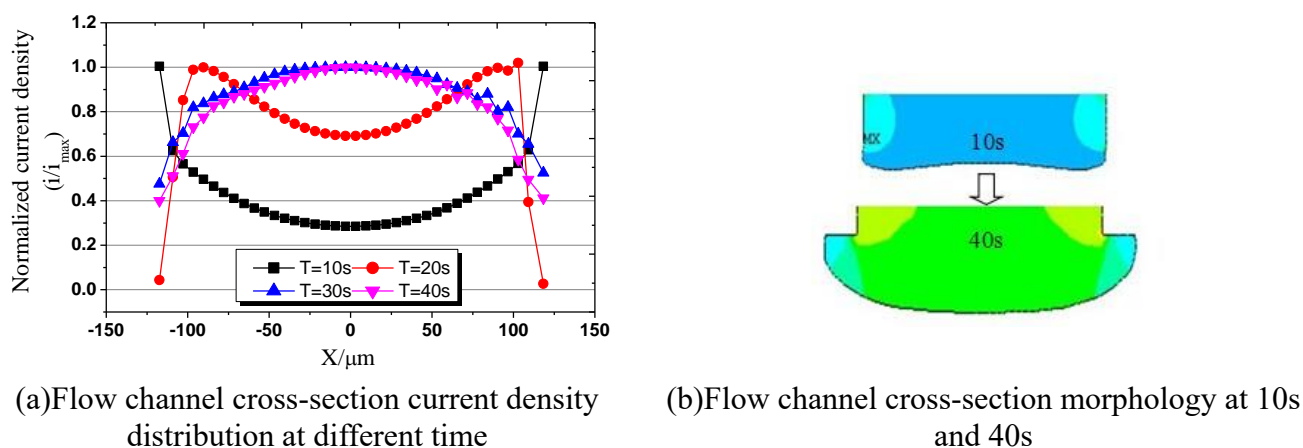


**Figure 3.** Change of flow channel cross-section morphology with the time by simulation

In this section, the experimental study was also carried out to verify the flow channel morphology changing with time. The channel morphology and the cross-section shapes are shown in Figure 4(a) at machining time of 5s. It is observed that the raised morphology appears at the central region in the bottom of the flow channel. It is because that the metal in the central region of the flow channel is dissolving more slowly than that at both bottom sides of the flow channel, which is as similarly demonstrated in the previous simulation results. In other word, the raised morphology appeared because the electric field was weak in the central region and was strong in both bottom sides of flow channels in the initial machining stage. This situation also appears when the TMEMM is used to generate micro-dimples, which is called “island”. Zhang[19] analyzed the reason by simulation which is also caused by the non-uniform electrical field and proposed multiple sandwich-like electrochemical micromachining (SLEMM) to eliminate the “island” phenomenon. At machining time of 20s, however, no raised morphology occurred in the flow channel, as shown in Figure 4(b), which indicated that the electric field of flow channels in the central region became stronger than that in both bottom sides as the machining was progressing, which was gradually eliminating the raised morphology in the central region. This experiment result was consistent with the simulation and analysis result presented previously.

The analysis of the experimental data was also carried out in this section. The variation of flow channels size and the calculated etching factor ( $EF$ ) with machining time are shown in Figure 4(c)(d). It is observed from the figures that the electrolyte is able to flow freely along the entire flow channels in the initial machining stage, which allows fast material removal in the width and depth directions of flow channels after a voltage is applied. As machining is progressing, the increasing depth of flow channels

creates resistances to the electrolyte renewal and more space between the cathode and the anode, which would slow the machining rate. In the other hand, the continuously increase of the lateral etching and the decrease of the etching rate in the depth direction lead to a continuous decrease of the etching factor and lower localization of the flow channels.

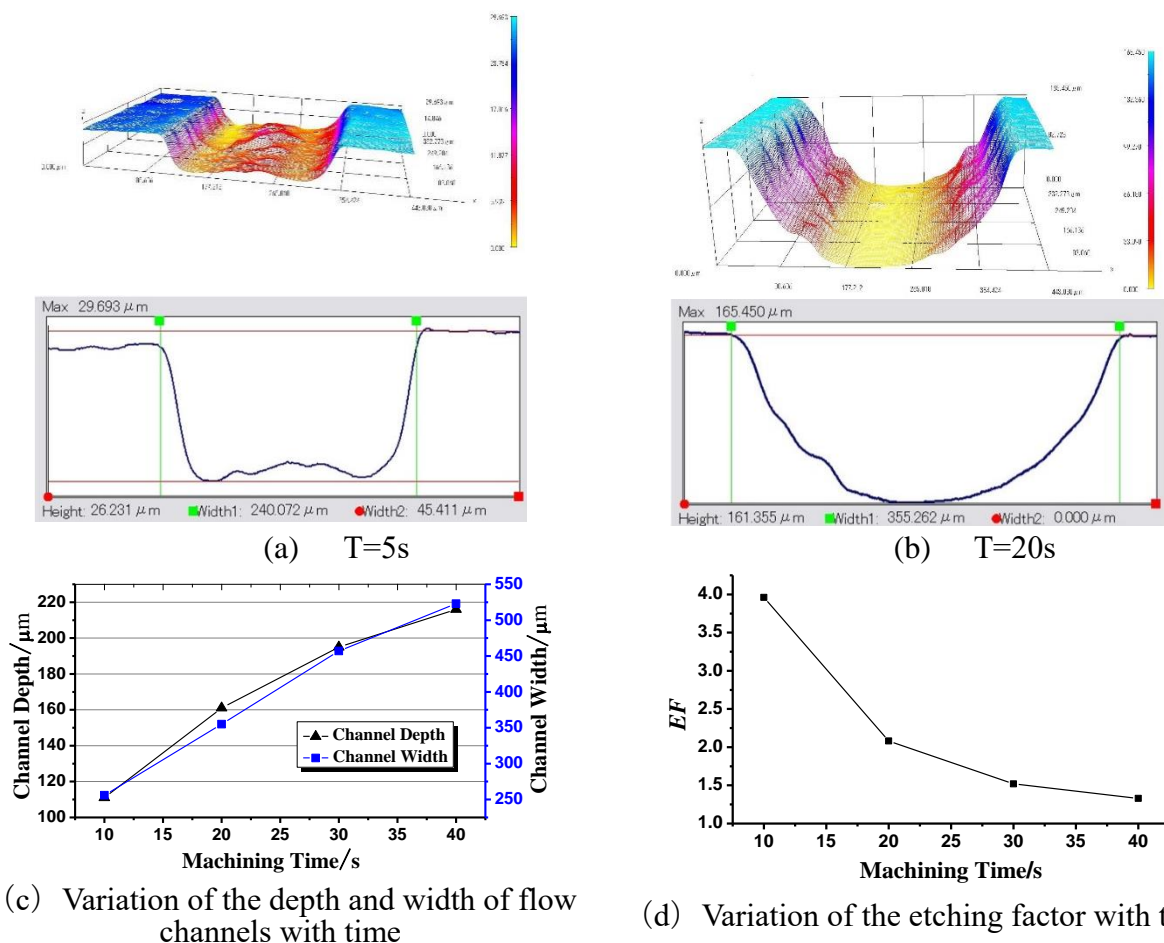


**Figure 4.** Flow channel cross-section morphology and the analysis of experimental data

### 3.2 Influence of pulse and DC power sources on the TMEMM

The pulse power source in electrochemical machining utilizes the intermittent pulses to provide the power to the enclosed machine region and the pulses can lead to some changes in physical and chemical properties of the electrolyte during the electrochemical machining between the electrodes. Li[20] found it useful to maintain smaller inter-electrode gaps to achieve better machining accuracy. Bhattacharyya[21] studied the application of the pulsed power can avoid problems of non-uniform dissolution of the anode work piece and reduce the temperature during the machining process. Unlike the conventional DC power source, the way of a pulse power source supplying power enables the material in the enclosed anode machining region to have the periodically discontinuous electrochemical dissolution reaction in the electrolyte which is beneficial to increase the mass transfer velocity and the uniformity of the electrical conductivity in the interelectrode gap. In addition, the use of the pulse power

source allows to intensify the nonlinearity of the current efficiency and to expand the passivating dissolution region of the anode.

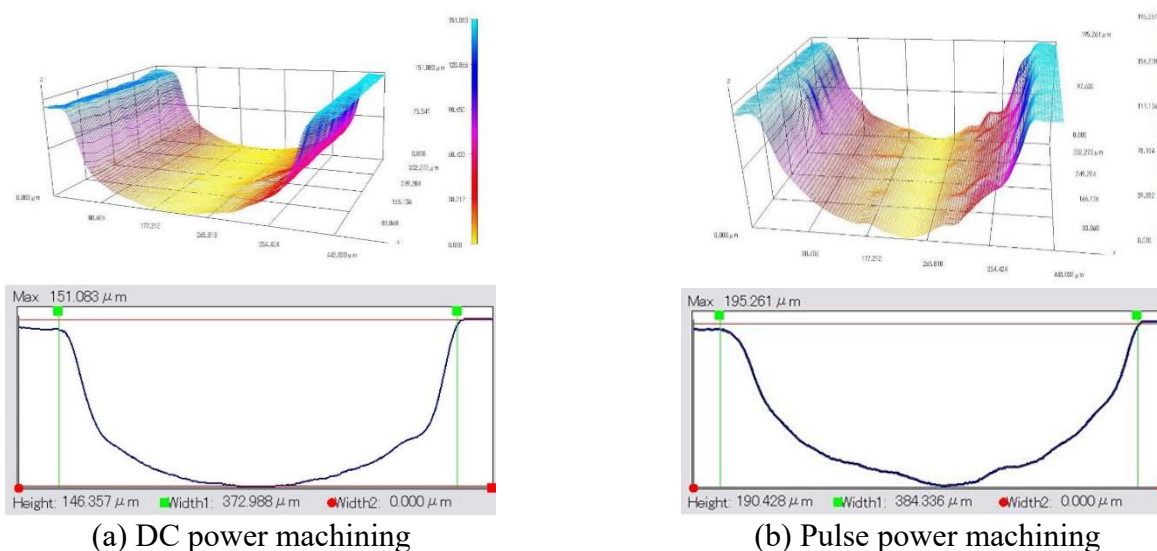


**Figure 5.** Flow channel morphology and 2D cross-section profile resulting from DC and pulse power machining

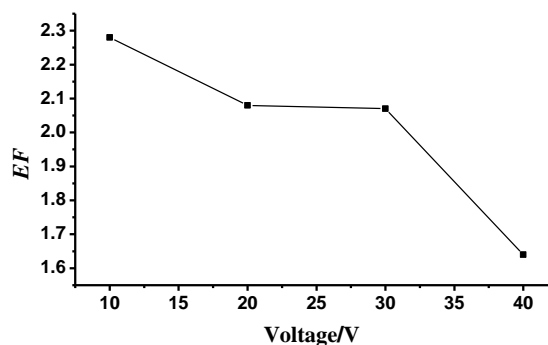
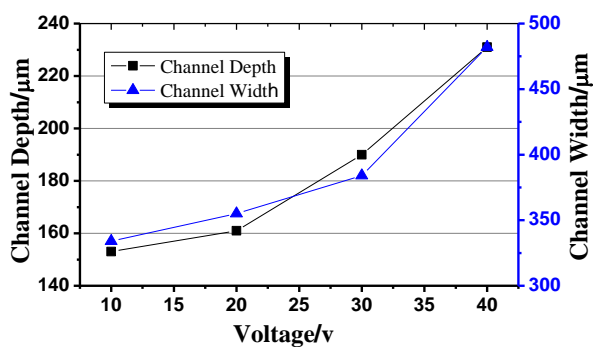
Both DC and pulse power sources were used in the experiment for the comparison purpose. The duty ratio of the pulse voltage used in the experiment was 50% and the frequency was 2 kHz. The flow channel cross-section morphologies resulting from the DC and pulse power sources are shown in Figures 5(a) and 5(b), respectively. The cross-section dimensions in the depth and width directions are then measured from the morphology shown in Figure 5 and the etching factors are also calculated, as listed in Table 1. Within the same electrochemical machining time, the depth and width of the flow channel as well as the etching factor using the pulse power source are greater than those using the DC power source. It shows that the constant updating of electrolyte in the electrodes gap can enhance polarization and reduce lateral corrosion obviously. Therefore, when the pulse power source is used during machining, the electrolyte can be renewed in time to improve the efficiency in electrochemical machining, to weaken dispersive etching and to improve the machining localization.

**Table 1.** The flow channels depth, width and etching factor resulting from both DC and pulse power machining sources

Power source	Voltage U/V	Flow channel depth/ $\mu\text{m}$	Flow channel width/ $\mu\text{m}$	EF
DC power source	30	146	373	1.69
Pulse power source	30	190	384	2.07

### 3.3 Influence of the average current density on the TMEMM

It is known from the electrochemical machining theory that the anode material removal rate is proportional to the machining current density. The influence of different machining current densities on the electrochemical machining flow channels is evaluated in this study. When the pulse power source is used in machining, the current density is generally represented by the average current density. The cross-section morphologies of the electrochemical machining flow channel using voltage, respectively, at 10V, 20V, 30V and 40V along with the corresponding average current density, respectively at  $14.8\text{A}/\text{cm}^2$ ,  $16.0\text{A}/\text{cm}^2$ ,  $17.0\text{A}/\text{cm}^2$  and  $23.1\text{A}/\text{cm}^2$  are used in the experiment. The corresponding measured cross-section widths and depths of the flow channel along with the calculated etching factors for those 4 conditions are shown in Figures 6(a) and 6(b), respectively.



(a) Dependence of flow channel width and depth on the pulse voltage

(b) Dependence of the etching factor on the pulse voltage

**Figure 6.** The analysis of experimental data

It is seen from Figure 6(a) that the width and depth of the flow channel steadily increase as the voltage and the average current density increase, which indicates that the machining material removal rate in the width and depth directions increases clearly with an increased voltage and the average current density. When the voltage increases from 10V to 30V, the etching factor only drops slightly. For the voltage between 20V and 30V, the etching factor remains almost unchanged, which indicates that the voltage in this range has little influence on the localization of the electrochemical machining. When the voltage increases from 30V to 40V; however, the etching factor drops rapidly which indicates that the localization falls rapidly when the machining voltage is more than 30V. Obviously, when the current density reaches a certain value and then continues to rise, the corrosion rate of each spot in the flow channel also increases rapidly, which will increase lateral corrosion and reduce the *EF*. Therefore, a voltage between 20V and 30V should be selected for flow channels electrochemical machining for greater machining efficiency and better machining localization.



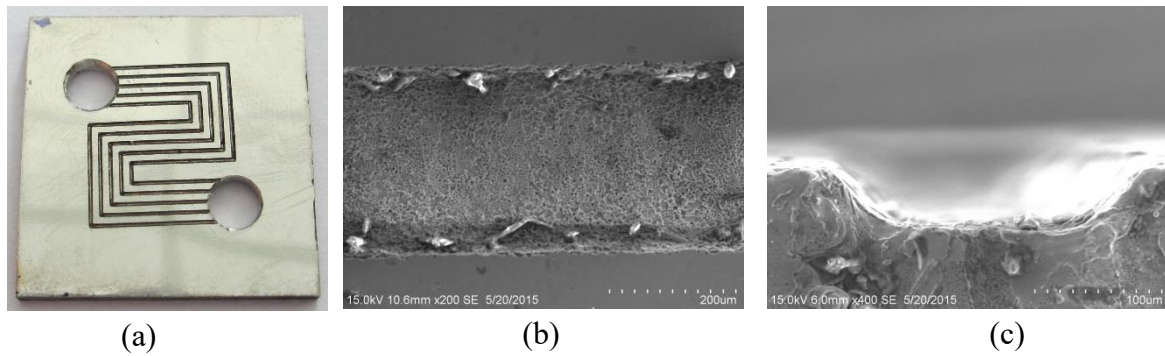


**Figure 7.** An example of flow channels from electrolysis machining at 20V pulse voltage

Based on the above results, the adoption of a pulse voltage between 20V and 30V can improve the electrochemical machining efficiency and localization and prolonging the machining time can eliminate any central raised morphology in flow channels. As an example, the machined test sample surface, the top surface morphology and the cross-section morphology of the flow channel resulting from electrochemical machining using a pulse power source with the voltage at 20V and the machining time at 20s are shown, respectively in Figures 7(a), 7(b) and 7(c).

#### 4. CONCLUSIONS

The TMEMM was adopted to process the micro channel structures in metal bipolar plates and the corresponding finite element analysis model was built to analyze the forming process of microchannel cross-sections. The experimental study was also carried out to machine metal surface microchannel structures using the TMEMM in the designed machining platform. Experimental results showed that the TMEMM could be used to effectively process microchannels in metal surfaces and the use of a pulse voltage between 20V and 30V can dramatically improve the machining efficiency and localization.

#### ACKNOWLEDGEMENT

This work was financially supported by the National Natural Science Foundation of China (grant no.51305212) and the Research Fund of Nantong University Xinglin college (grant no.2018K124), the Priority Academic Program Development of Jiangsu Higher Education Institutions and Qing Lan Project of Jiangsu Province.

#### References

1. H. Tawfik, Y Hung, D Mahajan, *J. Power Sources*, 163 (2007) 755.
2. S. Karimi, N. Fraser, B. Roberts, *Adv. Mater. Sci. Technol.*, 2012 (2012) 1.
3. S. Shimpalee, V. Lilavivat, H. Mccrabb, *Int. J. Hydrogen Energy*, 41 (2016) 13688.
4. J. Wang, J. Sun, L. Song, *Int. J. Hydrogen Energy*, 37 (2012) 1140.
5. Y. Liu, H. Lin, *J. Power Sources*, 195 (2010) 3529.

6. J. H. Kim, S. K. Kim, Y. Z. You, D.I. Kim, S.T. Hong, H.C. Suh and K. Scott Weil, *Int. J. Electrochem. Sci.*, 6 (2011) 4365.
7. S. J. Lee, C. Y. Lee, K. T. Yang, F. H. Kuan, P.H. Lai, *J. Power Sources*, 185 (2008) 1115.
8. J. C. Hung, D. H. Chang, Y. Chuang, *J. Power Sources*, 198 (2012) 158.
9. K. P. Rajurkara, M. M. Sundaramb, A. P. Malshec, *Procedia CIRP*, 6 (2013) 13.
10. C. H. Jo, B. H. Kim, C. N. Chu, *CIRP Ann.*, 58 (2009) 181.
11. J. W. Byun, H. S. Shin, M. H. Kwon, B. H. Kim and C. N. Chu, *Int. J. Precis. Eng. Manuf.*, 11 (2010) 747.
12. Y. Liu, H. T. Cai, H. S. Li, *J. Manuf. Process.*, 17 (2015) 162.
13. C. Madore, O. Piotrowski, D. Landolt, *J. Electrochem. Soc.*, 146 (1999) 2526.
14. X. L. Chen, N. S. Qu, H. S. Li, Z. Y. Xu, *J. Mater. Process. Technol.*, 229 (2016) 102.
15. N. S. Qu, X. L. Chen, H. L. Li, Y. B. Zeng, *Chin. J. Aeronaut.*, 27 (2014) 1030.
16. X. F. Zhang, N. S. Qu, X. L. Chen, *Surf. Coat. Technol.*, 302 (2016) 438.
17. D. Zhu, N. S. Qu, H. S. Li, Y. B. Zeng, D. L. Li, S. Q. Qian, *CIRP Ann.*, 58 (2009) 177.
18. X. Y. Wang, X. L. Fang, Y. B. Zeng, N. S. Qu, *Int. J. Electrochem. Sci.*, 11 (2016) 7216.
19. X. F. Zhang, H. Li, Z. Yin, R. Kun, *Int. J. Electrochem. Sci.*, 14(2019)427.
20. X.H.Li, Z.L.Wang, W.S.Zhao, f.Q.Hu, *Key Engineering Materials*, 339(2007)327.
21. B.Bhattacharyya, B. Doloi, P.S.Sridhar, *J. Manuf. Process.*,(1-3)(2001)301.

© 2019 The Authors. Published by ESG ([www.electrochemsci.org](http://www.electrochemsci.org)). This article is an open access article distributed under the terms and conditions of the Creative Commons Attribution license (<http://creativecommons.org/licenses/by/4.0/>).